International Journal of Thin Films Science and Technology

http://dx.doi.org/10.18576/ijtfst/130103

Adsorption of Eriochrome Black-T dye by batch investigations using waste tea@Fe NPs as low-cost adsorbent

Rehana B. Mampilly[1], Sandip H. Bhatt[2], Niral J. Modi[3], and Amanullakhan Pathan[4,]*

[1]Government Polytechnic, Raska, (Mehmadabad), Kheda -387120, Gujarat Technological University, Ahmedabad, India
[2]Chemical Engineering Department, L.D college of Engineering, Gujarat Technological University, Ahmedabad, India
[3]Government Engineering College, Sector-29, Gandhinagar-382030, Gujarat Technological University, Ahmedabad, India
[4]Shri Sarvajanik (PG) Science College, Mehsana-384001, Hemchandracharya North Gujarat University, Patan, India

Received: 22 Aug. 2023, Revised: 23 Sep. 2023, Accepted: 14 Oct. 2023.
Published online: 1 Jan. 2024.

Abstract: This work has examined the efficaciousness of iron nanoparticles made from tea waste extract in the elimination of Eriochrome black T (EBT) dye. Field emission gun scanning electron microscopy (FEG-SEM) with EDAX, High-resolution transmission electron microscopy (HR-TEM), X-ray diffraction (XRD), and FTIR spectroscopy were used to evaluate the synthesized iron capped nanoparticles. Iron nanoparticles seemed amorphous, according to the X-ray diffraction patterns. The spherical form of the Fe NPs was discernibly shown by scanning electron microscopy. Particle size of Fe NPs is found to be in the 30–40 nm range using transmission electron microscopy (HR-TEM). Additionally, research was done on the deterioration of the Eriochrome black T pigment (EBT). It was investigated how several experimental factors, such as the amount of adsorbent, pH, dye concentration, and contact duration, affected the pace of reaction in order to determine the ideal conditions for dye degradation. There are pseudo-first-order kinetics involved in the adsorption of the dye Eriochrome black T (EBT). At a pH of 3, 50 ppm of Eriochrome Black T (EBT) dye concentration, and 0.60 g of adsorbent, the dye degradation was observed to exhibit optimized results. The highest dye elimination was accomplished by stirring for 90 minutes at a Room temperature.

Keywords: Adsorption, Iron Nanoparticles, XRD, FTIR, FE-SEM, EDAX, HR-TEM.

1 Introduction

One of the main issues facing the modern world is environmental pollution. The textile industry spends a lot of time dying fabrics, which at various points during the dyeing and finishing processes contaminates a lot of water with dyes. Dyes are used in a number of different industries, including food processing, leather, paper, pulp mills, cosmetics, and printing [1]. An estimated 10,000 distinct types of dyes are produced annually by 7.0×105 tonnes of various enterprises globally. During the dyeing process, between 1 and 15% of these colours are lost as effluents [2]. Dyes, or synthetic colourants made from organic sources, have been connected to mutagenic and carcinogenic consequences [4], as well as surface and groundwater pollution [3]. Because certain artificial colours don't decompose naturally, they can be extremely dangerous to aquatic life. By obstructing sunlight, they can lower the quantity of photosynthetic activity in water plants. This state may impair the re-oxygenation of the water, which might impede the proper development of aquatic organisms [5]. Azole dyes account for more than 70% of all synthetic dyes used by the global dyeing industry. A reactive azo dye's molecular structure has one or more azo groups (-N=N-) that serve as chromophores [6]. Furthermore, even at low concentrations, the majority of synthetic dyes are made up of molecules with an azo group, which are resistant to heat, light, chemicals, and microbial destruction [7]. Consequently, it is now imperative to eliminate these synthetic dyes prior to discharging spent industrial wastewater into the water system. Many attempts have been undertaken to remove dyes from wastewaters using commonly used techniques such photocatalytic degradation [8,9], photo-Fenton reaction [10], biodegradation, solvent extraction, coagulation, precipitation, membrane filtering, and advanced oxidation processes [11,12]. Because of their larger surface area and enhanced adsorption capacity, nanoparticles (NPs) have been assumed to be the most effective adsorbents [13]. Iron-based nanoparticles, or Fe-NPs, have been used in groundwater treatment and the cleanup of previous sites recently because to their larger surface area and high efficiency [14]. Fe-NPs can be easily made by physical and chemical processes, but these approaches have limitations that are not discussed in this work, such as the need for dangerous substances like sodium borohydride (NaBH4) and the usage of organic solvents, dispersions, stabilising agents, and stabilising agents. An increasing number of studies are synthesizing Fe-NPs from waste tea extract in an economical and environmentally benign manner [16]. Among the conventional methods used to remove dyes from wastewater are photocatalytic degradation [17–22], biological treatment [23–25], chemical coagulation [24–26], cation exchange membranes [25–27],

*Corresponding author E-mail: amankhan255@gmail.com

electrochemical degradation [26–27], chemical-biological degradation, photo-Fenton reaction [28–29], and advanced oxidation process [29]. While these methods yield positive results, the preparation and execution of the materials need a significant amount of labour. Moreover, a number of secondary pollutants that are more dangerous than the initial chemical are produced during photocatalytic breakdown, such as various oxidative intermediates. Conversely, adsorption processes are simpler, easier to implement, and easier to carry out on a large scale. Previous research has looked at the production of magnetic nanoparticles from tea debris and their application in the removal of arsenic and nickel from aqueous solutions [30, 31]. The present study, in contrast to prior studies, used Fe-NPs generated from discarded tea extracts to remove PR from an aqueous solution. Recently, plant extracts [32–38], black tea, green tea leaves, and waste tea [30, 39, 40] have all been used to produce iron nanoparticles. All of the study, however, was built around the creation of Fe-nanoparticles using waste tea. A very successful attempt was made in the current study to use waste tea for the first time in the synthesis of Fe-NPs.

This study looks at how iron nanoparticles made from Waste tea extract may remove the color Eriochrome black T (EBT). FTIR spectroscopy, X-ray diffraction (XRD), High-resolution transmission electron microscopy (HR-TEM), and Field emission gun scanning electron microscopy (FEG-SEM) with EDAX were used to evaluate the synthesized iron capped nanoparticles. Additionally, the study examined the deterioration of Eriochrome black T (EBT) dye. The influence of several experimental factors, such as the fraction of adsorbent, pH, dye concentration, and contact duration on the pace of reaction, was explored in order to determine the ideal conditions for dye degradation.

2. Experimental:

2.1 Materials:

AR grade ferrous sulfate and Eriochrome black T (EBT) dye were used as received from the *s.d*. fine chemicals (India) and used without further purification. Waste tea were purchased from the market. All the solutions were prepared in double distilled water.

2.2 Synthesis of Iron nanoparticles:

The Waste tea extracts were prepared by adding 60 gm tea into 1000 ml distilled water and heating them at 353 K for 60 min in a water bath and the extracts were vacuum filtered. After cooling to the room temperature, then 0.10 mol/L $FeSO_4$ solutions was added to the Waste tea extracts with a ratio volume of 1:2. The Fe nanoparticles were formed when black Fe NPs were observed in the solution mixed Fe (II) and Waste tea extracts. The resulting solution was centrifuged for 20 min; the supernatant was discarded, and the pellets were washed 3 times with distilled water to remove unreacted salts and tea phytochemicals on the colloidal surface. Following a final wash, the WT@iron particles were centrifuged, the supernatant was discarded, and particles were dried in an oven.

2.3 Adsorption activities:

In order to gauge the synthetic iron nanoparticles' adsorption capacity, Eriochrome black T (EBT) decolorization was observed. An anionic dye called eriochrome black T (EBT) is widely used in the printing and dyeing industries. It is extremely harmful to human health. Even though the adsorption of Eriochrome black T (EBT) using various reductants has been extensively studied, it is interesting to investigate the ecologically safe iron nanoparticles. Eriochrome black T (EBT) solution and iron nanoparticles interacted at various pH (2.0–10.0), adsorbent amounts, dye concentrations, and contact times. The Eriochrome black T (EBT) dye solution was equally divided between two beakers for the adsorption tests, which were conducted under various settings.

a. The first beaker containing Eriochrome black T (EBT) dye solution and WT@iron nanoparticle at room atmosphere without sunlight.

b. The second beaker containing Eriochrome black T (EBT) dye solution and iron nanoparticle with sunlight.

Using a chilled circulating liquid bath, the reaction temperature was maintained at 29±1oC. To achieve adsorption-desorption equilibrium between the dye solution and the adsorbent surface, 200 mL of the dye solution of the appropriate concentration—which included the desired amount of the adsorbent (0.1 to 1.0 g) and a predetermined amount of 2 mM NaOH solution and HCl (for pH)—was magnetically stirred before the irradiation experiments. The solution was also left in the dark for at least 15 minutes. Subsequently, the irradiation was initiated and the first sample (at 0 min) was removed. Samples of 5–10 mL were taken during the irradiation process at regular intervals (every 15 minutes), centrifuged, and the supernatant was then examined. As the irradiation period increased, the dye aliquots' absorbance was monitored at its λmax (538 nm). The absorbance spectra that were seen align with the Beer-Lambert Law within the dye concentration range that was investigated. A standard calibration curve that was derived using the dye's absorbance at several known concentrations was used to calculate the dye's concentration. To ensure that the experimental results could be replicated, the adsorption experiments were conducted three times. It was discovered that the absorbance was accurate to within ± 2. The recycling trials examined the adsorbent's uniformity in activity. Centrifugation was used to recover the adsorbent following the initial attempt at the adsorption experiment. Ethanol and deionized water were used to completely wash the recovered adsorbent. After 12 hours of drying at 60 degrees Celsius, the adsorbent was utilised again in the following adsorption experiment cycle. In a similar manner, a series of cycles of the experiment were conducted to track the adsorbent's decrease in efficiency following repeated usage.

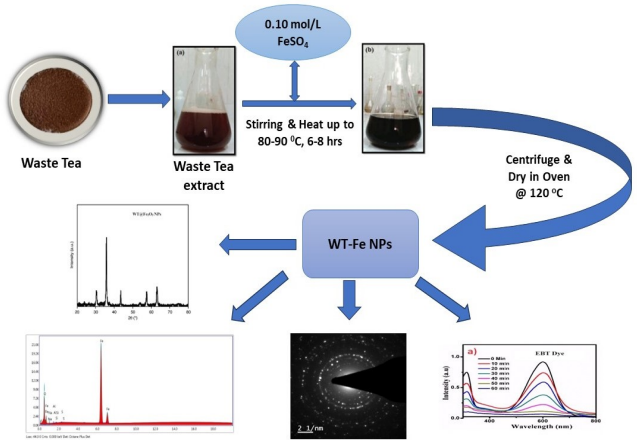

Fig. 1: Schematic diagram of WT@Fe nanoparticles.

The removal efficiency (%) was calculated as follows:

$$\textit{Degradation}\ (\%) = \frac{C_0 - C}{C_0} \times 100 \ldots\ldots\ldots \quad (1)$$

Where C_0 is the initial concentration of Eriochrome black T (EBT), and C is the time-dependent concentration of dye upon irradiation of visible light. The following first-order kinetic equation can be used to describe the removal of Eriochrome black T (EBT).

$$ln\left(\frac{C_0}{C_t}\right) = kt \ldots\ldots\ldots\ldots\ldots \quad (2)$$

Where C_0 and Ct are the concentrations of dye in solution at times 0 and t respectively, and k is the first-order rate constant (sec-1).

3. Results and Discussion:

3.1 Characterization of iron nanoparticles:

3.1.1 FTIR spectra of iron nanoparticles:

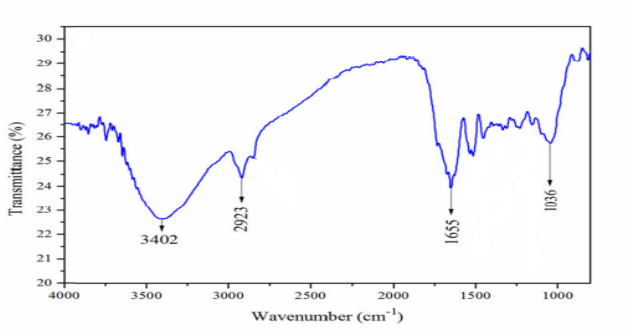

Fig. 2: FTIR spectra of (a) Iron nanoparticles before adsorption of EBT).

The Fe-capped waste tea nanoparticles comprised a range of functional groups, as seen by the FT-IR spectra (Fig. 2). The broad band at 3402 cm-1 reflected the bound –OH groups. The alkane functional groups' -C-C stretching is what produced the peaks at 2923 and 2853 cm-1. Similarly, the aromatic functionality and -C=C stretching vibration may be responsible for the band at around 1655 cm-1. The two bands, at 1146 and 1036 cm-1, were assigned to the C-O and C=O groups, respectively [41-42].

3.1.2 X-ray diffraction (XRD) spectra of iron nanoparticles:

The Fe Nanoparticles' XRD patterns, which were created using waste tea extracts, are displayed in Figure 3. Based on the spectrum data, zero-valent iron (α-Fe), maghemite (α-Fe2O3), magnetite (Fe3O4), and iron hydroxides were identified as the peaks in XRD patterns with 2θ values of 62.800, 57.30, 43.9º, 36.48º, and 30.60º [43, 44]. However, because the Fe NPs produced by Waste tea extract were amorphous in form, iron oxides and iron oxohydroxides were mostly found instead of Fe0 [45]. The organic component polyphenols/caffeine from Waste tea extract was found as the intensity peak at 2θ = 22.36º [46,47].

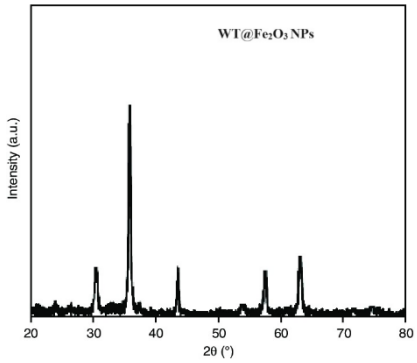

Fig. 3: X-ray Diffraction spectra of (a) Iron capped tea waste Nanoparticles:

3.1.3 Field emission gun scanning electron microscope (FEG-SEM) of iron nanoparticles:

Scanning electron microscopy (SEM) was used to analyse the surface morphology of iron nanoparticles. SEM micrographs of the iron nanoparticle samples are displayed in Figure 4. Figure 4 depicts the Fe NPs prior to their interaction with Eriochrome black T (EBT), confirming their spherical form and diameter range of 30–40 nm. Iron and oxygen element peaks may be seen in the EDAX spectra of Fe capped nanoparticles, showing that the particles are developing well. The elements have peak indexes of 0.5 keV for oxygen and 6.4 and 7.2 keV for iron. Oxygen makes up 30.53% of the elements' mass proportion, whereas iron makes up 62.72%.

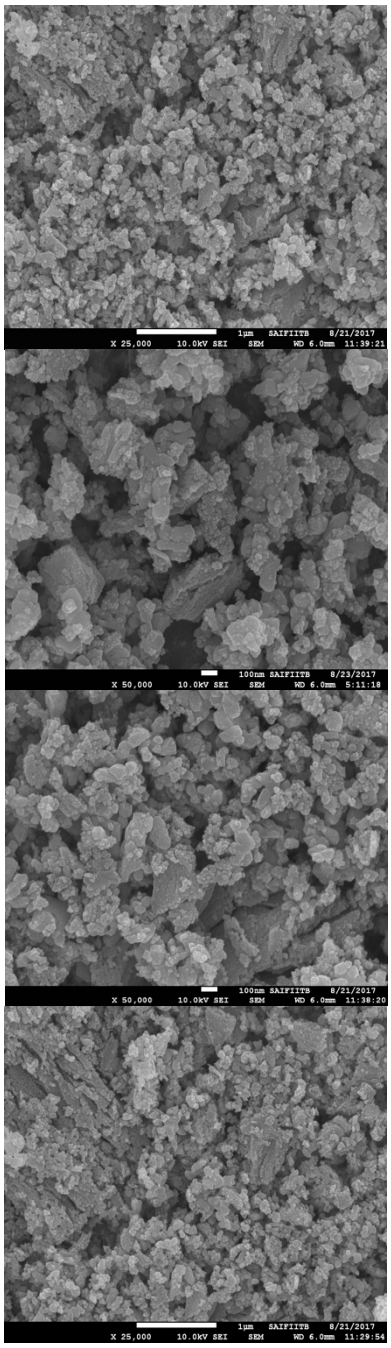

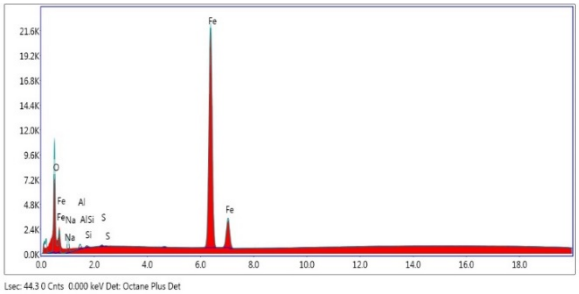

Fig. 4: FE-SEM of Iron Nanoparticles with EDAX

3.1.4 High resolution transmission electron microscope (HR-TEM) of iron nanoparticles:

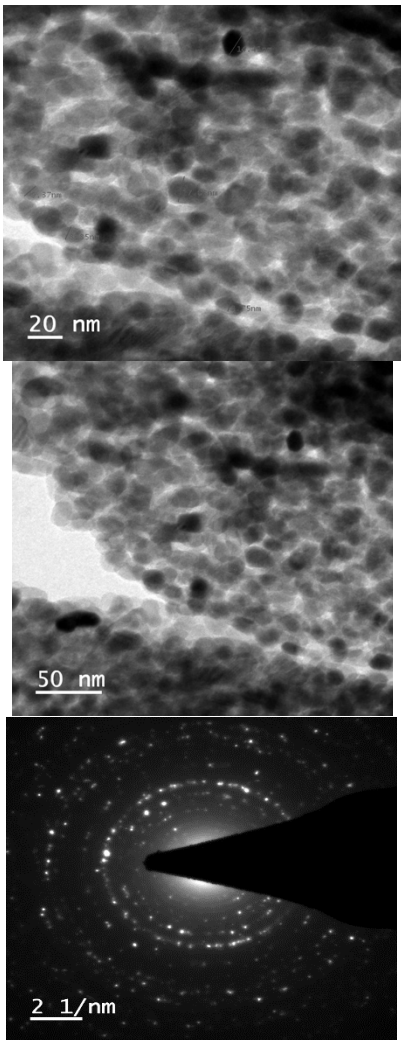

Fig. 5: HR-TEM images of iron nanoparticles:

The HR-TEM image of iron nanoparticles is displayed in Figure 5. HR-TEM pictures demonstrating that most of the particles had a homogeneous shape, had a circular morphology, and ranged in size from 30 to 40 nm. A bright circular spot selected area electron diffraction (SAED) pattern was used to show the crystallinity of the Fe capped nanoparticles.

3.2 Various Parameters Which Effects on Eriochrome black T (EBT) Dye adsorption in the presence of Iron Nanoparticles:

3.2.1 Effect of adsorbent dosage:

Different concentrations of iron nanoparticles were used since their use is expected to change the dye degradation process.

The proportion of Eriochrome black T (EBT) removal increased together with the amount of adsorbent dosage.

This is because the adsorption active site is more accessible and the iron surface area is larger. Nevertheless, the rate stabilised almost immediately with the addition of a specific quantity of adsorbent (0.60 g). This may be the result of the adsorbent's exposed surface area (active sites) not growing with increased adsorbent concentration beyond a certain threshold. Only the layer's thickness rose when the adsorbent coated the reaction tank's bottom. It's conceivable that an adsorbent quantity-related impact was not discovered when a saturation threshold was achieved.

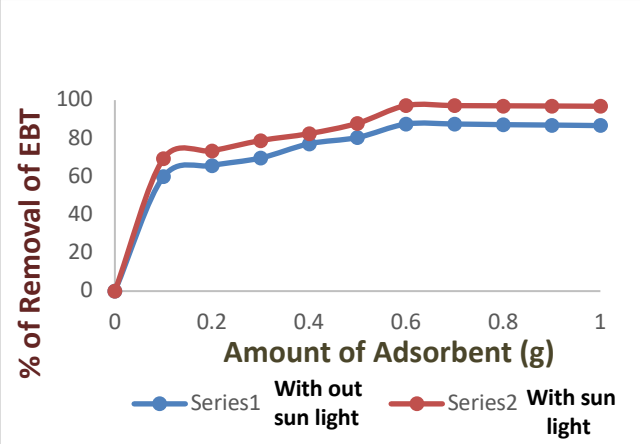

Fig. 6: Effect of adsorbent dosage on the adsorption of Eriochrome black T (EBT) by WT@iron nanoparticles

Additionally, the utilization of different-sized reaction containers corroborated this notion. The adsorbent exposed surface grew together with the vessel's bottom area, increasing the percentage of dye removal. In the current investigation, identical-sized beakers were utilised for the whole experiment. Additional adsorbent addition did not improve the % of dye removal; instead, it only increased the layer thickness after a maximum exposure to adsorbent. The testing findings showed that the highest removal % of Eriochrome black T (EBT) dye could be achieved using 0.60 g of adsorbent.

3.2.2 Effect of pH:

One of the most significant factors affecting the dye removal process for water treatment is the initial pH value since it may alter the charge of a surface on both dye molecules and adsorbent in an aqueous solution. Current studies look at how adsorption is affected by the pH of the dye solution. The studies were conducted at a constant temperature of 29±1ºC, with an adsorbent dose of 0.60 g and an adsorbate concentration of 50 ppm. A pH range of 2 to 10 was used to assess the dye's adsorption, and the pH was changed by adding 0.1M HCl or 0.1M NaOH. Eriochrome black T (EBT) is a cationic dye that takes the form of positively charged ions in an aqueous solution. Since it is a charged ion, the pH of the solution primarily influences the surface charge of the adsorbent, which in turn affects the degree of its adsorption onto the surface of Fe NPs.

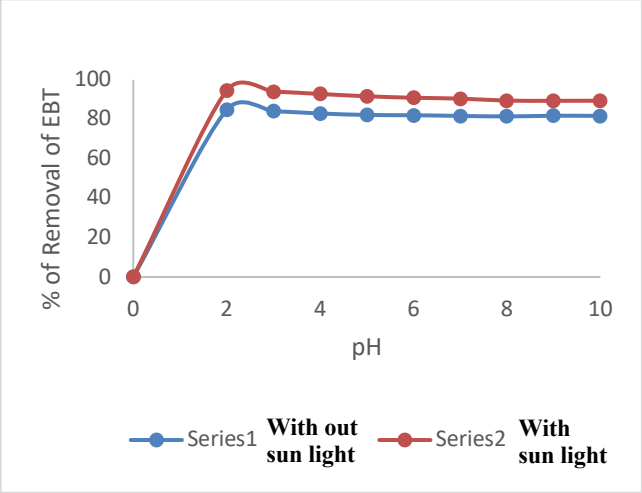

Fig. 7: Effect of pH on the adsorption of Eriochrome black T (EBT) by WT@iron-nanoparticle

The obtained data are shown in Figure 7, which indicates that adsorption of eriochrome black T (EBT) rises with rising pH from 2.0 to 7.0 and that the % of removal of eriochrome black T (EBT) starts to decrease as pH climbs further. The reason for this is because as pH rises, the surface activity of Fe NPs shift from positive to negative charge, which causes an electrostatic contact to occur between the adsorbent and the molecules of Eriochrome black T (EBT). when can be shown in Figure 7, the percentage of dye removed decreases when pH increases from 2 to 7 and increases from 3 to 10. Eriochrome black T (EBT) was most maximally absorbed by WT@iron nanoparticles at pH 2.0. With WT@Fe2O3 NPs, the maximum degradation of Eriochrome black T (EBT) dye was around 94.56 percent.

3.2.3 Effect of concentration:

It has been shown that the equilibrium adsorption rises when the starting concentration of Eriochrome black T (EBT) increases from 50 ppm to 250 ppm. The results are explained by the fact that more Eriochrome black T (EBT) adsorption results from an increase in the mass transfer driving force, which happens when the starting concentration increases. Additionally, it was shown that when the initial concentration of Eriochrome black T (EBT) dye increases, the proportion of dye eliminated reduces. As seen in Figure 8, the highest percentage of dye removed by WT@Fe nanoparticles in a 50-ppm solution of Eriochrome black T (EBT) dye was 96.30%.

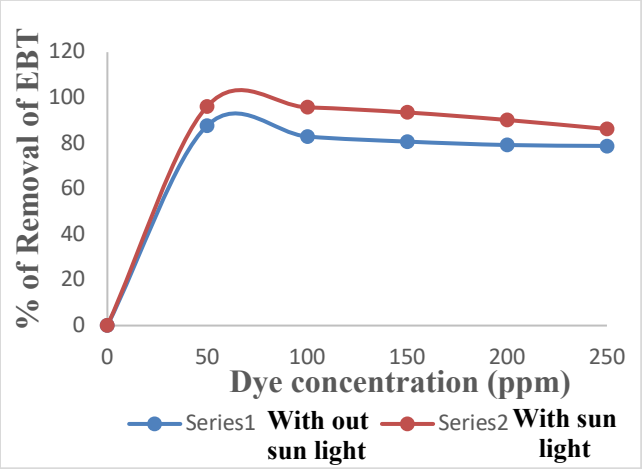

Fig. 8: Effect of concentration on the adsorption of Eriochrome black T (EBT) by WT@iron nanoparticles

3.2.4 Effect of Contact Time:

The impact of contact time is the most important factor in the elimination of adsorption dye. Every experiment was run for a predetermined amount of time. Figure 9 illustrates the relationship between contact time and the Eriochrome black T (EBT) dye's efficacy in dye removal. It is evident that as contact length grows, so does the percentage of dye removal. Within a predetermined time frame, the impact of contact time on the removal of Eriochrome black T (EBT) dye was examined. Figure 9 shows how contact time affects the adsorbent's ability to remove Eriochrome black T (EBT) dye.

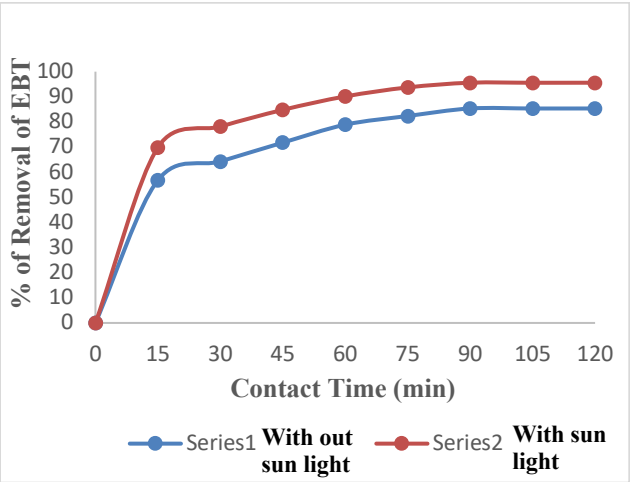

Fig. 9: Effect of contact time on the removal of EBT by WT@iron-nanoparticles.

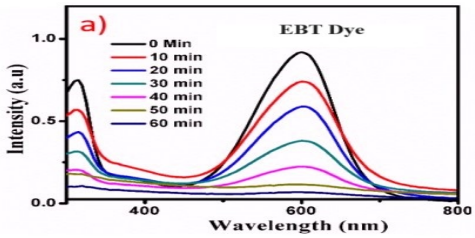

Fig. 10: UV-Vis absorption spectra for degradation of Eriochrome black T (EBT) dye in the presence of Fe capped tea waste Nanoparticles.

The availability of a significant number of unoccupied sites for Eriochrome black T (EBT) adsorption can be attributed to the rapid adsorption at initial contact time, but the sluggish rate of dye adsorption could be related to slow pore diffusion of the dye into the bulk adsorbent. Maximum dye removal was achieved at 90 minutes utilizing WT@Fe NPs, which was approximately 95.85 percent.

4. Conclusion:

Iron nanoparticles derived from black tea waste were used to remove the Eriochrome black T (EBT) dye. The synthesized iron nanoparticles were characterized using X-ray diffraction (XRD), scanning electron microscopy, FTIR spectroscopy, and high-resolution transmission electron microscopy (HR-TEM) (FE-SEM). The X-ray diffraction patterns demonstrated the amorphous nature of iron nanoparticles. It was simple to see that Fe NPs were spherical using scanning electron microscopy. Fe NPs identified by hydrogen radiation microscopy (HR-TEM) had particle sizes of 30–40 nm. UV-visible absorption spectroscopy was also utilised to monitor the deterioration of Eriochrome black T (EBT) dye using iron nanoparticles. The ideal parameters for dye degradation were found by examining changes in temperature, pH, and adsorbent concentration. The effects of dye concentration and contact duration on reaction rate were examined analytically. We noticed that the adsorption of the dye Eriochrome black T (EBT) followed pseudo-first-order kinetics. For optimal dye degradation outcomes, eriochrome black T (EBT) dye at a concentration of 50 ppm, pH = 2, and 0.60 g of adsorbent were required. The greatest degree of dye removal was attained after 90 minutes of stirring at 29±1ºC. WT@iron nanoparticles were added, and it was found that 95.85% of the colour was removed.

References:

[1] Monvisade, P., & Siriphannon, P. (2009). Chitosan intercalated montmorillonite: Preparation, characterization and cationic dye adsorption. *Applied Clay Science*, *42*(3-4), 427-431.

[2] Barka, N., Abdennouri, M., & Makhfouk, M. E. (2011). Removal of Methylene Blue and Eriochrome

Black T from aqueous solutions by biosorption on Scolymus hispanicus L.: Kinetics, equilibrium and thermodynamics. Journal of the Taiwan Institute of Chemical Engineers, 42(2), 320-326.

[3] Mohammadi, N., Khani, H., Gupta, V. K., Amereh, E., & Agarwal, S. (2011). Adsorption process of methyl orange dye onto mesoporous carbon material–kinetic and thermodynamic studies. Journal of colloid and interface science, 362(2), 457-462.

[4] Lin, S. H., Juang, R. S., & Wang, Y. H. (2004). Adsorption of acid dye from water onto pristine and acid-activated clays in fixed beds. Journal of hazardous materials, 113(1-3), 195-200.

[5] Ejhieh, A. N., & Khorsandi, M. (2010). Photodecolorization of Eriochrome Black T using NiS–P zeolite as a heterogeneous catalyst. Journal of Hazardous Materials, 176(1-3), 629-637.

[6] Ahmad, A. A., & Hameed, B. H. (2010). Fixed-bed adsorption of reactive azo dye onto granular activated carbon prepared from waste. Journal of hazardous materials, 175(1-3), 298-303.

[7] Gerçel, Ö., Gerçel, H. F., Koparal, A. S., & Öğütveren, Ü. B. (2008). Removal of disperse dye from aqueous solution by novel adsorbent prepared from biomass plant material. Journal of Hazardous Materials, 160(2-3), 668-674.

[8] Sun, J., Qiao, L., Sun, S., & Wang, G. (2008). Photocatalytic degradation of Orange G on nitrogen-doped TiO2 catalysts under visible light and sunlight irradiation. Journal of hazardous materials, 155(1-2), 312-319.

[9] García-Montaño, J., Ruiz, N., Munoz, I., Domenech, X., García-Hortal, J. A., Torrades, F., & Peral, J. (2006). Environmental assessment of different photo-Fenton approaches for commercial reactive dye removal. Journal of hazardous materials, 138(2), 218-225.

[10] Azmi, W., Sani, R. K., & Banerjee, U. C. (1998). Biodegradation of triphenylmethane dyes. Enzyme and microbial technology, 22(3), 185-191.

[11] Crini, G. (2006). Non-conventional low-cost adsorbents for dye removal: a review. Bioresource technology, 97(9), 1061-1085.

[12] Robinson, T., Chandran, B., & Nigam, P. (2002). Removal of dyes from a synthetic textile dye effluent by biosorption on apple pomace and wheat straw. Water research, 36(11), 2824-2830.

[13] Nayak, T., & Pathan, A. (2023). Environmental remediation and application of carbon-based nanomaterials in the treatment of heavy metal-contaminated water : A review. Materials Today: Proceedings.

[14] Shi, L. N., Zhang, X., & Chen, Z. L. (2011). Removal of chromium (VI) from wastewater using bentonite-supported nanoscale zero-valent iron. Water research, 45(2), 886-892.

[15] Huang, L., Weng, X., Chen, Z., Megharaj, M., & Naidu, R. (2014). Synthesis of iron-based nanoparticles using oolong tea extract for the degradation of malachite green. Spectrochimica Acta Part A: Molecular and Biomolecular Spectroscopy, 117, 801-804.

[16] Shahwan, T., Sirriah, S. A., Nairat, M., Boyacı, E., Eroğlu, A. E., Scott, T. B., & Hallam, K. R. (2011). Green synthesis of iron nanoparticles and their application as a Fenton-like catalyst for the degradation of aqueous cationic and anionic dyes. Chemical Engineering Journal, 172(1), 258-266.

[17] Pathan, A. A., Desai, K. R., & Bhasin, C. P. (2017). Improved Photocatalytic Properties of NiS Nanocomposites Prepared by Displacement Method for Removal of Rose Bengal Dye. Current Nanomaterials, 2(3), 169-176.

[18] Vajapara, S., Patel, S., & Bhasin, C. (2017). Efficient Adsorption and Photocatalytic Degradation of Malachite Green Dye Using Bentonite Natural Adsorbent. Int. J. Nano. Chem, 3(2), 33-37.

[19] Desai, K. R., Pathan, A. A., & Bhasin, C. P. (2017). Synthesis, characterization of cadmium sulphide nanoparticles and its application as photocatalytic degradation of congored. Int J Nanomater Chem, 3, 39.

[20] Vajapara, S., Pathan, A., & Bhasin, C. P. (2023). Adsorption and Photocatalytic Performance of Activated Carbon and Activated Carbon-La2O3 nanoparticles Composites for Malachite Green. Int. J. Thin. Film. Sci. Tec, 12(1), 21-37.

[21] Pathan, A. A., Prajapati, C. G., Dave, R. P., & Bhasin, C. P. (2022). Effective and Feasible Photocatalytic Degradation of Janus Green B dye in Aqueous Media using PbS/CTAB Nanocomposites. Int. J. Thin. Fil. Sci. Tec, 11(2), 245-255.

[22] Pathan, A. A., Bhatt, S. H., Vajapara, S. J., & Bhasin, C. P. (2022). Solar Light Induced Photo Catalytic Properties of α-Fe2O3 Nanoparticles for Degradation of Methylene Blue Dye. Int. J. Thin. Fil. Sci. Tec, 11(2), 213-224.

[23] Alinsafi, A., Da Motta, M., Le Bonté, S., Pons, M. N., & Benhammou, A. (2006). Effect of variability on the treatment of textile dyeing wastewater by activated sludge. Dyes and Pigments, 69(1-2), 31-39.

[24] Selcuk, H. (2005). Decolorization and detoxification of textile wastewater by ozonation and coagulation

processes. Dyes and pigments, 64(3), 217-222.

[25] Wu, J. S., Liu, C. H., Chu, K. H., & Suen, S. Y. (2008). Removal of cationic dye methyl violet 2B from water by cation exchange membranes. Journal of membrane science, 309(1-2), 239-245.

[26] Fan, L., Zhou, Y., Yang, W., Chen, G., & Yang, F. (2008). Electrochemical degradation of aqueous solution of Amaranth azo dye on ACF under potentiostatic model. Dyes and pigments, 76(2), 440-446.

[27] Sudarjanto, G., Keller-Lehmann, B., & Keller, J. (2006). Optimization of integrated chemical–biological degradation of a reactive azo dye using response surface methodology. Journal of hazardous materials, 138(1), 160-168.

[28] Hameed, B. H., & Daud, F. B. M. (2008). Adsorption studies of basic dye on activated carbon derived from agricultural waste: Hevea brasiliensis seed coat. Chemical Engineering Journal, 139(1), 48-55.

[29] Wu, F. C., & Tseng, R. L. (2008). High adsorption capacity NaOH-activated carbon for dye removal from aqueous solution. Journal of hazardous materials, 152(3), 1256-1267.

[30] Panneerselvam, P., Morad, N., & Tan, K. A. (2011). Magnetic nanoparticle (Fe3O4) impregnated onto tea waste for the removal of nickel (II) from aqueous solution. Journal of hazardous materials, 186(1), 160-168.

[31] Lunge, S., Singh, S., & Sinha, A. (2014). Magnetic iron oxide (Fe3O4) nanoparticles from tea waste for arsenic removal. Journal of Magnetism and Magnetic Materials, 356, 21-31.

[32] Lunge, S., Singh, S., & Sinha, A. (2014). Magnetic iron oxide (Fe3O4) nanoparticles from tea waste for arsenic removal. Journal of Magnetism and Magnetic Materials, 356, 21-31.

[33] Shahwan, T., Sirriah, S. A., Nairat, M., Boyacı, E., Eroğlu, A. E., Scott, T. B., & Hallam, K. R. (2011). Green synthesis of iron nanoparticles and their application as a Fenton-like catalyst for the degradation of aqueous cationic and anionic dyes. Chemical Engineering Journal, 172(1), 258-266.

[34] Smuleac, V., Varma, R., Sikdar, S., & Bhattacharyya, D. (2011). Green synthesis of Fe and Fe/Pd bimetallic nanoparticles in membranes for reductive degradation of chlorinated organics. Journal of membrane science, 379(1-2), 131-137.

[35] Kuang, Y., Wang, Q., Chen, Z., Megharaj, M., & Naidu, R. (2013). Heterogeneous Fenton-like oxidation of monochlorobenzene using green synthesis of iron nanoparticles. Journal of colloid and interface science, 410, 67-73.

[36] Kharissova, O. V., Dias, H. R., Kharisov, B. I., Pérez, B. O., & Pérez, V. M. J. (2013). The greener synthesis of nanoparticles. Trends in biotechnology, 31(4), 240-248.

[37] Makarov, V. V., Makarova, S. S., Love, A. J., Sinitsyna, O. V., Dudnik, A. O., Yaminsky, I. V., ... & Kalinina, N. O. (2014). Biosynthesis of stable iron oxide nanoparticles in aqueous extracts of Hordeum vulgare and Rumex acetosa plants. Langmuir, 30(20), 5982-5988.

[38] Lin, J., Weng, X., Jin, X., Megharaj, M., Naidu, R., & Chen, Z. (2015). Reactivity of iron-based nanoparticles by green synthesis under various atmospheres and their removal mechanism of methylene blue. RSC advances, 5(87), 70874-70882.

[39] PATEL, S. J., VAJAPARA, S., & BHASIN, C. Removal of Methylene Blue from Aqueous Solution by Synthesized Iron Nanoparticles using Black Tea. Chemical Science, 2020(9), 1.

[40] Mampilly, R. B., Pathan, A., & Bhasin, C. P. (2023). Visible Light-Assisted Degradation of Malachite Green dye using Waste Tea-Mediated Zinc Nanoparticles. Int. J. Thin. Film. Sci. Tec, 12(1), 39-51.

[41] Mampilly, R. B, Pathan, A., Prajapati, C.G., & Bhasin, C. (2021). Iron Capped Spent Tea Leaves as Nano-Adsorbent for Removal of Eriochrome Black T from Aqueous Phase. Asian Journal of Chemistry, 34(7), 1814-1820.

[42] Lin, J., Weng, X., Jin, X., Megharaj, M., Naidu, R., & Chen, Z. (2015). Reactivity of iron-based nanoparticles by green synthesis under various atmospheres and their removal mechanism of methylene blue. RSC advances, 5(87), 70874-70882.

[43] Chen, Z. X., Jin, X. Y., Chen, Z., Megharaj, M., & Naidu, R. (2011). Removal of methyl orange from aqueous solution using bentonite-supported nanoscale zero-valent iron. Journal of colloid and interface science, 363(2), 601-607.

[44] Chen, Z. X., Cheng, Y., Chen, Z., Megharaj, M., & Naidu, R. (2012). Kaolin-supported nanoscale zero-valent iron for removing cationic dye–crystal violet in aqueous solution. Journal of Nanoparticle Research, 14(8), 1-8.

[45] Shahwan, T., Sirriah, S. A., Nairat, M., Boyacı, E., Eroğlu, A. E., Scott, T. B., & Hallam, K. R. (2011). Green synthesis of iron nanoparticles and their application as a Fenton-like catalyst for the degradation of aqueous cationic and anionic dyes. Chemical Engineering Journal, 172(1), 258-266.

[46] Colon, M., & Nerin, C. (2012). Role of catechins in the antioxidant capacity of an active film containing green tea, green coffee, and grapefruit extracts. Journal of agricultural and food chemistry, 60(39), 9842-9849.

[47] Hoag, G. E., Collins, J. B., Holcomb, J. L., Hoag, J. R., Nadagouda, M. N., & Varma, R. S. (2009). Degradation of bromothymol blue by 'greener'nano-scale zero-valent iron synthesized using tea polyphenols. Journal of Materials Chemistry, 19(45), 8671-8677.